

Journal Pre-proofs

Development of celecoxib-derived antifungals for crop protection

Yihui Ma, Lirong Yang, Xiuxiu Liu, Jun Yang, Xianglong Sun

PII: S0045-2068(19)31461-0

DOI: <https://doi.org/10.1016/j.bioorg.2020.103670>

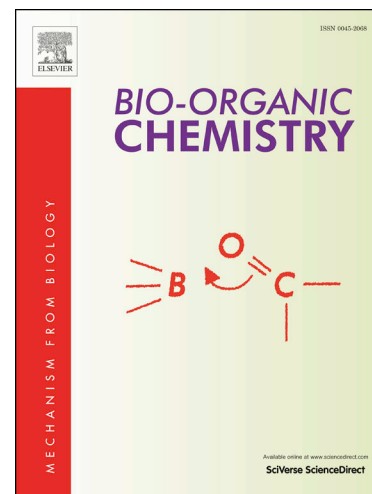
Reference: YBIOO 103670

To appear in: *Bioorganic Chemistry*

Received Date: 5 September 2019

Revised Date: 7 February 2020

Accepted Date: 14 February 2020



Please cite this article as: Y. Ma, L. Yang, X. Liu, J. Yang, X. Sun, Development of celecoxib-derived antifungals for crop protection, *Bioorganic Chemistry* (2020), doi: <https://doi.org/10.1016/j.bioorg.2020.103670>

This is a PDF file of an article that has undergone enhancements after acceptance, such as the addition of a cover page and metadata, and formatting for readability, but it is not yet the definitive version of record. This version will undergo additional copyediting, typesetting and review before it is published in its final form, but we are providing this version to give early visibility of the article. Please note that, during the production process, errors may be discovered which could affect the content, and all legal disclaimers that apply to the journal pertain.

Development of celecoxib-derived antifungals for crop protection

Yihui Ma^{a*}, Lirong Yang^a, Xiuxiu Liu^a, Jun Yang^a, Xianglong Sun^a,

^a Plant Protection Institute, Henan Academy of Agricultural Sciences, Zhengzhou
450002, China

Address for Correspondence:

Yihui Ma, PhD

Plant Protection Institute, Henan Academy of Agricultural Sciences

Zhengzhou 450002, China PR

Tel: 86-371-65731656

Email: ma.150@buckeyemail.osu.edu

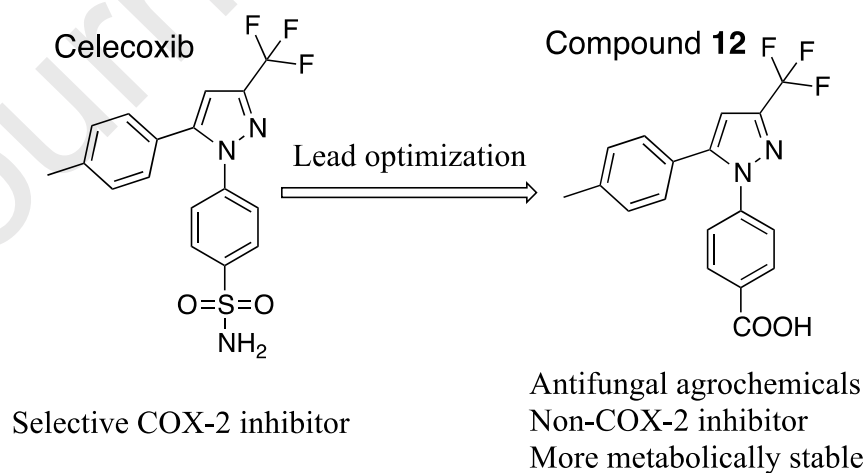
Abstract

Selective COX-2 inhibitor celecoxib was found directly inhibiting the growth of tested phytopathogenic fungi with the inhibitory rate ranging from 30-40% at 100 µg/ml. Lead optimization of celecoxib led to the identification of compound **12** among its derivatives as the most active antifungal candidate. The antifungal effect of compound **12** was supposed to be independent of COX-2 inhibition. Transcriptome profiling analysis of *Fusarium graminearum* (PH-1) treated with compound **12** brought about 406 up-regulated and 572 down-regulated differentially express genes (DEGs) respectively.

Keywords

Celecoxib; COX-2 inhibitor; lead optimization; antifungal agrochemical

Graphical abstract



Highlight

- Cyclooxygenase-2 (COX-2) selective inhibitor, celecoxib, was found directly inhibiting the growth of phytopathogenic fungi at concentrations over 100 µg/ml.
- Derivation of celecoxib leads to the identification of compound 12, a non-COX-2 inhibitor with increased antifungal activity.
- Transcriptome profiling analysis of compound 12 treated *Fusarium graminearum* (PH-1) revealed 406 up-regulated and 572 down-regulated differentially expressed genes (DEGs) respectively.
- These DEGS were enriched and cofactor binding was the most enriched gene ontology (GO) category.

Introduction

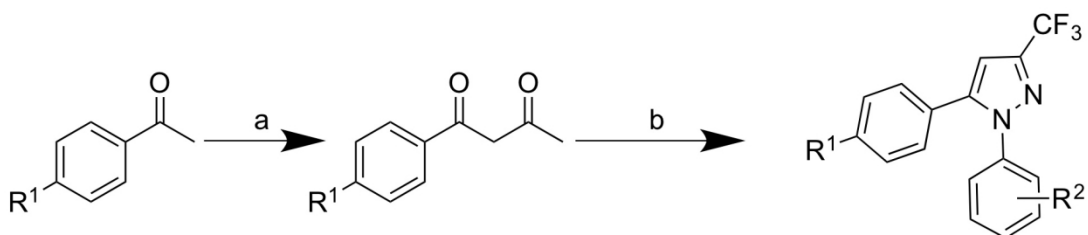
Phytopathogenic fungi are responsible for a wide range of serious plant disease and can cause destructive impact to major crops such as wheat, rice and maize [1, 2]. The majority of plant diseases are caused by fungi pathogens. Generally, crop disease control relies heavily on chemical fungicides and fungicides treatment represents an effective approach among the strategies for the plant disease management. Unlike previously used inorganic fungicides, recently developed fungicides features lower application rates, less phytotoxicity and easier to apply by farmers, representing a major improvement in antifungal pesticide discovery. Since their introduction, significant progress on the research as well as development of a variety of fungicides with different modes of action have been seen, due to the rapid growth of the fungicide markets. Recently, hundred of thousands tons of fungicides in active ingredients have been used annually [3]. However, long-term and intensive application of these chemical fungicides have exerted high selective pressure in pathogenic fungi and increased the risks of resistance development [4-8]. Indeed, many cases of resistance to almost each class of fungicides with various mode of action have been documented. Thus develop fungicides with unique structures and/or novel mode of action is greatly desirable to combat fungicide resistance.

Pyrazole motif is a very useful structural unit for molecule design in medicinal chemistry and frequently present in both agrochemicals and pharmaceuticals [9, 10]. Pyrazole derivatives are well-known for their broad-spectrum of biological activities such as anti-inflammatory[11], anti-analgesic[12], antifungal[13] and anticancer effect [14]. Celecoxib, a pyrazole derivative, is a COX-2 selective nonsteroidal anti-inflammatory drug (NSAID) used to treat pain or inflammation caused by many conditions such as arthritis and menstrual pain [12]. Besides, celecoxib also exhibited off-target activity such as antibacterial [15-18] and anticancer effect [19]. And many active antibiotics and anticancer agents with higher level of activity than celecoxib have been under development by structural optimization of celecoxib's scaffold. In addition, celecoxib was also reported to reduce the fungal burden in the lungs and spleen of mice infected with *Histoplasma capsulatum* as well as increased the survival of mice after infection with a lethal inoculum of *H. capsulatum* [20]. Interestingly, this apparent antifungal activity was still mediated through its effect against COX-2 and the subsequent inhibition of prostaglandins. Thus, direct effect of celecoxib against fungal pathogens has not been well explored. Inspired by the broad-spectrum biological activities of celecoxib which may arise from its versatile 1,5-diaryl-3-trifluoromethyl skeleton, and in the continuation of our current effort to seek antifungal chemicals for crop protection, it is very interesting to profile the antifungal activity of celecoxib against some representative plant pathogenic

fungi and further explore the potential of this unique scaffold to develop practically effective fungicides through structural optimization. In this study, celecoxib was found moderately active against four selected species of fungi phytopathogens. Lead optimization of celecoxib for more potent fungicidal pesticides gave rise to 19 analogs, which were screened for their antifungal activity. Among them, compounds **12**, which has a -COOH in the *para* position of the phenyl ring attached to the N1 atom of the pyrazole, demonstrates the enhanced activity over celecoxib and was more active than any other members in the library.

Chemistry:

The synthesis of compounds 1-19 was following the scheme 1. Generally, acetophenones were condensed with ethyl trifluoroacetate in anhydrous tetrahydrofuran with sodium hydride as base to give 1,3-dione adducts, which was cyclized with various substituted phenylhydrazine hydrochloride in ethanol to give corresponding final compounds. Compounds 12, 18 and 19 which bear a free -COOH were prepared in N,N-dimethylformide to avoid the formation of corresponding ethyl ester. All the compounds were characterized with ^1H ^{13}C NMR and HRMS. The spectroscopic data (supplementary materials) was in full accordance with their depicted structures and consistent with those reported [12].



R¹ = F; OMe and Me

R² = 2-Cl; 3-Cl; 4-Cl; 2,4-dichlor; 2,6-dichloro; 4-Br; 4-F; 2,4-difluoro; 2-NO₂; 4-NO₂; 4-OMe; 4-COOH; 4-CN; 4-OCF₃; 2-CH₃; 4-CF₃ and 4-SO₂Me

(a) ethyl trifluoroacetate, NaH/THF; (b) substituted phenylhydrazine-HCl, EtOH, reflux.

Scheme 1 Synthetic route to compound 1-19.

Result and Discussion

Celecoxib exhibited broad-spectrum antifungal effect against tested phytopathogenic fungi.

To examine whether celecoxib has any antifungal activity, potato agrose dishes (PDA) assay was used to test its inhibitory effect on the growth of four selected species of pathogenic fungi available in our lab at a broad concentration range across 0.1, 1, 10, 100 µg/ml and the results is depicted in figure 1. Interestingly, our results revealed that celecoxib, a selective COX-2 inhibitor, exhibited moderate but clear inhibition against each tested pathogens. Starting 1 µg/ml, celecoxib showed slight activity against *Fusarium graminearium Seh*w and *Myrothecium roridum* with the inhibition of 14% and 9% respectively. The inhibitory rate rose to 20%-30% at concentration of 10 µg/ml against all the

tested fungi except for *Helminthosporium maydis* Nisik & Miy which did not demonstrated any susceptibility to celecoxib at this concentration. In contrast, 100 µg/ml celecoxib obviously inhibited the growth of *Helminthosporium maydis* Nisik & Miy with an inhibition of 50%, indicating the sensitivity of this fungi to the tested concentrations. There was also slight improvement in potency for celecoxib at 100 µg/ml against the other three fungi with the enhanced inhibition rate of 30-40% compared to that at 10 µg/ml. Further increasing celecoxib's concentration up to 400 µg/ml did not bring about significant improvement in inhibition (data not shown). Even though, this observed direct inhibition effect associated with celecoxib is different from its host-directed antifungal effect against *Histoplasma capsulatum* infection, which also resulted from its original COX-2 inhibition property. Thus, this finding underscores the potential of celecoxib acting as a lead compound to develop novel antifungals for agricultural purpose.

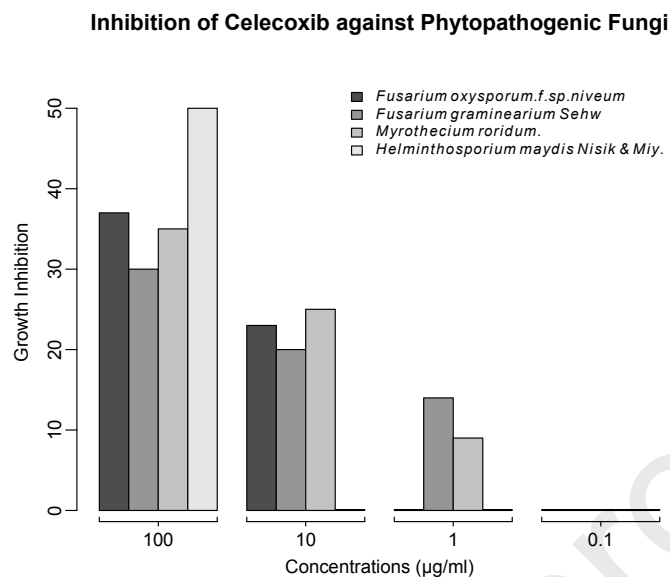


Fig 1. The effects of lead compound celecoxib on four species of crop pathogens were measured using PDA assay at concentrations of 0.1,1,10,100 µg/ml.

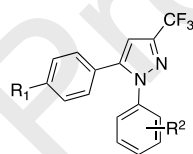
Exploration the Antifungal Activity of celecoxib Derivatives

Encouraged by the above-described findings of the direct antifungal activity of celecoxib against phytopathogenic fungi, we performed lead optimization by exploiting its scaffold as a molecular platform to develop potent antifungal agrochemicals for crop protection. Accordingly, we designed and synthesized a focused compound library consisting of 19 derivatives of celecoxib. At first, to examine the steric and electronic effect of the substituents on the phenyl group attached to the N1 of pyrazole ring on fungicidal activity, substituents with various bulkiness and electron properties were introduced to generate compound 1-17. SAR analysis revealed an exclusive preference to $-COOH$ among various

substituents in R1 as compound **12** exhibited higher level of activity against each fungus than any other members within the compound series and noticeable potency improvement relative to lead compound celecoxib. For example, the inhibition of compound **12** against *Fusarium oxysporum.f.sp.niveum*, *Fusarium graminearium* Sehwa and *Myrothecium roridum* reached 83%, 84% and 73%, comparing to the respective inhibition rates of 37%, 30%, and 35% associated with celecoxib. It is also encouraging that the growth of *Helminthosporium maydis* Nisik & Miy was completely inhibited by compound **12**. However, the results for the rest analogues were disappointing as they generally displayed much lower level of potency regardless of substitution patterns. Interestingly, further optimization of toluene moiety revealed there is certain flexibility in selecting R2, as either electron-donating or electron-withdrawing functional group apparently both elevated the antifungal activity of the corresponding compound **18** and **19** compared to celecoxib. And between them, compound **18** demonstrated slightly more promising antifungal effect than that of compound **19**. On the other hand, *Myrothecium roridum* was most susceptible to these chemicals and several derivatives including compound **8**, **11**, **12**, all revealed similar inhibition rate over 70%. While for the most tolerable strain *Helminthosporium maydis* Nisik & Miy, none of these analogues displayed any inhibition rate greater than 17% with the exception of compound **12**, **18** and **19**, which by contrast greatly inhibited its growth. Compared to two controls,

compound **12** demonstrated comparable antifungal potency with that of triadimenfon, but was still less active than pyraclostrobin, which completely inhibited the growth of all the tested fungi. Even though, the increased antifungal activity of compound **12** over the lead compound celecoxib indicated that celecoxib could be structurally optimized to develop potent antifungals and its 1,5-diaryl scaffold may represent a novel potential pharmacophore for antifungals development by appropriately selecting the substituents on the two aromatic rings.

Table 1. Inhibition rate of celecoxib and its derivatives against fungi pathogens at 100 mg/ml.



Compounds	R ¹	R ²	% Growth Inhibition			
			<i>Fusarium oxysporum</i> f.s <i>p.niveum</i>	<i>Fusarium graminearum</i> <i>Sehw</i>	<i>Myrothecium roridum</i>	<i>Helminthosporium maydis</i> <i>Nisik & Miy</i>
celecoxib			37%	30%	35%	50%
1	Me	2-Cl	24%	29%	55%	0%
2	Me	3-Cl	14%	21%	36%	0%
3	Me	4-Cl	24%	36%	45%	15%
4	Me	2,4-dichloro	19%	21%	36%	17%
5	Me	2,6-dichloro	19%	21%	55%	0%

6	Me	4-Br	14%	36%	18%	0%
7	Me	4-F	24%	43%	64%	19%
8	Me	2,4-difluoro	19%	29%	71%	10%
9	Me	2-NO ₂	14%	43%	55%	0%
10	Me	4-NO ₂	24%	43%	73%	33%
11	Me	4-OMe	14%	29%	72%	0%
12	Me	4-COOH	83%	84%	73%	100%
13	Me	4-CN	10%	29%	27%	14%
14	Me	4-OCF ₃	0%	21%	18%	0%
15	Me	2-CH ₃	29%	29%	55%	17%
16	Me	4-CF ₃	5%	29%	55%	12%
17	Me	4-SO ₂ Me	29%	36%	73%	0%
18	4'-F	4-COOH	68%	57%	66%	60%
19	4'-OMe	4-COOH	57%	54%	56%	64%
Triadimefon			66%	100%	21%	33%
Pyraclostrobin			100%	100%	100%	100%

Differentially expressed genes (DEGs) in PH-1 was identified upon treatment of compound 12

As our initial attempt to explore the mode of action underlying the antifungal effect of compound 12, transcriptomic profiling analysis of *Fusarium graminearum* (PH-1) was employed to identify the differentially expressed genes after it was treated with compound 12. PH-1 was selected as a model

fungus for its genome has been extensively studied. RNA-seq expression profiling of PH-1 was performed 3h after treatment with 30 µg/ml of compound **12** to allow for the extraction of high quality RNA as any longer period of treatment and higher concentration of compound would further dissolve or inhibit the growth of hyphae. One biological replicate with paired-end was sequenced for compound **12**-treated PH-1 as well as the untreated. A total of 46413308 and 52319584 raw reads leading to 45510240 and 50755126 clean reads were collected from compound **12**-treated PH-1 as well as the untreated respectively (table 2).

Table 2 Transcriptome statistics of cDNA libraries from compound **12** treated PH-1 and untreated PH-1.

sample name	raw_reads ¹	clean_reads ²	clean_bases ³	error_rate ⁴	Q20 ⁵	Q30 ⁶	GC content ⁷
Comp. 12 treated PH-1	46413308	45510240	6.83G	0.03	97.72	93.69	54.13
Untreated PH-1	52319584	50755126	7.61G	0.03	97.85	93.97	54.01

1 The numbers of original data sequence

2 The filtered data sequence

3 $Q_{phred} = -10\log_{10}(e)$

4 The sequence length multiplied by the number of sequencing

5 The percentage of bases with a Phred value >20

6 The percentage of bases with a Phred value >30

7 The percentage of bases number of G and C

The sequence reads were mapped to the PH-1 genome (Table 3). Among the transcripts from two conditions, up to 97.01% and 97.2% of the total reads were

uniquely mapped to the PH-1 genome respectively. Small proportions (less than 0.5%) for both conditions were mapped to multiple locations in the PH-1 genome. All uniquely mapped reads were used to calculate FPKM (Fragments Per Kilobase Million), which can be used to normalize expression levels. Accordingly, Log2-fold DEGs between the two conditions were identified with corrected P-value of 0.05. A total of 978 DEGs were detected between compound **12**-treated and control, with 406 DEGs up-regulated and 572 down-regulated.

Table 3. Summary of mapping the sequenced reads to the PH-1 genome from compound **12** treated PH-1 and the untreated PH-1

Event of mapping	Sample	
	Comp. 12 treated PH-1	Untreated treated PH-1
Total reads	45510240	50755126
Total map ¹	44366473(97.49%)	49529691(97.59%)
Multi map ²	215899(0.47%)	196812(0.39%)
Unique map ³	44150574(97.01%)	49332879(97.2%)
Read1 map ⁴	22058738(48.47%)	24694718(48.65%)
Read2 map ⁵	22091836(48.54%)	24638161(48.54%)
Positive map ⁶	22044279(48.44%)	24644099(48.55%)
Negative map ⁷	22106295(48.57%)	24688780(48.64%)

¹Total number of reads mapped on the PH-1

²Total number of reads mapped to multiple locations in the PH-1

³Total number of reads mapped to uniquely locations in the PH-1

⁴The two directions of paired-end sequencing

⁵The two directions of paired-end sequencing

⁶Total number of reads mapped to positive strand of PH-1

⁷Total number of reads mapped to negative strand of PH-1

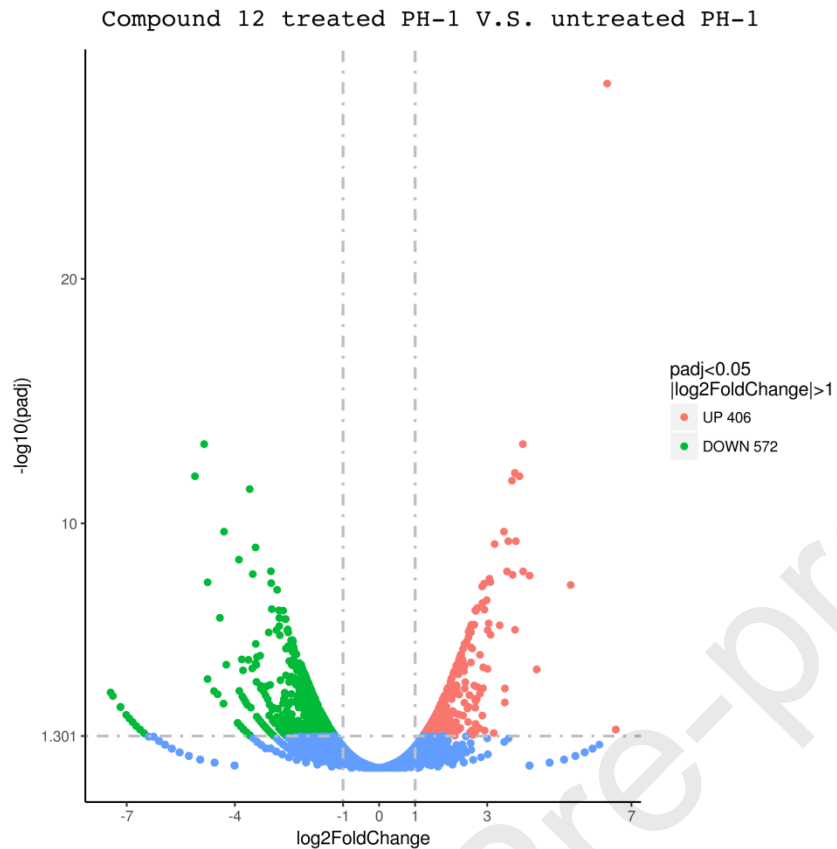


Fig 2. Volcano of DEGs between compound 12 treated PH-1 and untreated PH-1. The y-axis corresponds to the mean expression value of \log_{10} (p-value), and the x-axis displays the \log_2 fold change value. The red dots represent up-regulated DEGs, the green dots represent down-regulated DEGs.

The DEGs were then annotated and assigned to different functional GO (gene ontology) categories which fall into three groups of biological process (BP), cellular component (CC) and molecular function (MF). For each group, several most significant terms were

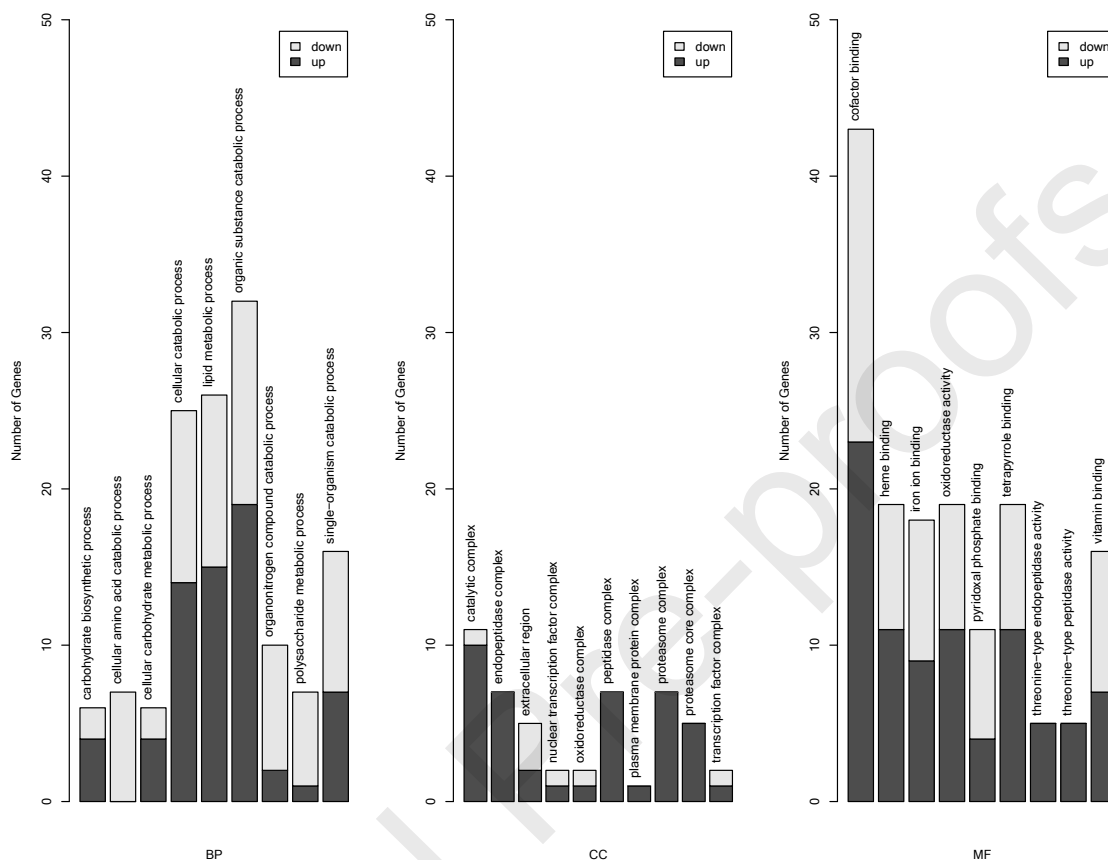


Fig 3. Functional annotation of DEGs based on gene ontology (GO) categorization.

depicted in figure 3. Specifically, for biological process, the dominant categories were organic substance catabolic process with 32 DEGs; catalytic complex had the most DEGs of 11 for the group cellular component. Notably, the largest category of cofactor binding in molecular function group was the most significant among all the gene categories in the gene enrichment analysis, indicating the importance of these pathway in the compound-12 induced antifungal effect.

Although many work still need to be done to explore the exact mode of action of compound 12, this assay provided global and useful information as to identify the direct target of this kind of antifungal chemicals.

Conclusion

Resistance development in phytopathogenic fungi has posed a big challenge for plant disease control and calls for novel types of fungicide for effective plant disease management. Keeping development of novel chemicals with highly potent activity or novel mode of action would always be awaited for resistance management. From drug development perspective, unique structure different from that of the currently used agrochemicals would have the potential to facilitate the fight against resistance. On the other hand, repurposing an existing drug to find new uses represent a promising alternative strategy for novel drug development in both pharmaceutical and agricultural area as it can accelerate the development process as well as reduces the research and development cost[21-24]. Here, we present that a widely used COX-2 inhibitor celecoxib showed direct antifungal effect on some selected phytopathogenic fungi. Structural modification led to the identification of compound 12 whose activity was significantly elevated over the lead compound celecoxib, and this improvement was closely related to the presence of the substituent of 4-COOH,

as any other substitution pattern did not deliver any apparent antifungal effect. More importantly, the structure of this kind of celecoxib-derived antifungal is different from any class of mainstream of fungicidal pesticides currently used in the market. Thus, this unique structure may be accompanied with novel mode of action, which would be instrumental to resistance management.

Regarding the mode of action, previous study showed that the COX-2 inhibition of compound 12 was significantly decreased compared to parent compound celecoxib [25], indicating the independence of the antifungal activity of these novel fungicides on their inhibition against COX-2. This promise was further confirmed by the lack of antifungal effect of compound 17, which is a potent COX-2 inhibitor with even longer plasma half-life [12]. Thus their putative antifungal target(s) must be different from COX-2-like enzyme in fungal pathogens. Our profiling analysis of compound 12's antifungal effect on PH-1 revealed that 406 differentially expressed gene were up-regulated while 572 down-regulated. All these DEGs were enriched and the result showed that cofactor-binding related DEGs were the most, followed by organic substance catabolic process. In contrast, cell component related DEGs were much less. Furthermore, it was reported that compound 12, with a carboxylic acid in the place of sulfonamide of celecoxib, showed higher level of metabolic stability that

that of celecoxib [25], suggesting compound **12** might have a longer duration of activity, which is a desirable property for their application in the field.

Although this work is about antifungal pesticides development, it may also have far-reaching implications in pharmaceutical areas. As celecoxib itself has been used in clinical for many years and in light of its outstanding physical properties, development of celecoxib-based fungicide to treat infectious disease may be a better start point due to the direct antifungal effect associated with its skeleton. In this context, it would be also interesting to examine as well the contribution resulted from the direct antifungal effect of celecoxib to the mice's defense improvement against *Histoplasma capsulatum* infection in addition to those mediated through host COX-2 inhibition[20].

Experiment

5.1 Chemistry

All chemical reagents were commercially available without further purification and flash column chromatography was performed over silica gel 200-300 mesh. Analytical thin-layer chromatography (TLC) was performed with silica gel plates using silica gel 60 GF254 (Qingdao Haiyang Chemical Co., Ltd). Melting points were determined with an X-4 melting points apparatus (Shanghai) and were uncorrected. High-resolution mass spectra were obtained on a Q-TOF Mass Spectrometer with ESI ionization. ¹H NMR and

^{13}C NMR spectra were recorded on a Bruker AM-400 spectrometer at 400 MHz and 100 MHz respectively. Chemical shifts are reported in parts per million relative to internal tetramethylsilane(TMS). All the tested compounds hold a purity of at least 95%. Analytical HPLC was performed on the Thermo Ultimate 3000 equipped with Thermo Scientific Acclaim-C18 column and UV wavelength set at 254 nm. Eluent: 40% MeOH in H_2O ; flow rate = 1 ml/min.

5.1.1 General procedure for the preparation of trifluoro-1-(4-substituted phenyl)butane-1,3-dione

To a tetrahydrofuran solution of acetophenones (100 mmol) was added NaH (200 mmol), and the mixture was stirred for 5 min. Ethyl trifluoroacetate (250 mmol) was then added. The reaction mixture was stirred at room temperature for 4 h and neutralized with 2N HCl. The precipitate formed was collected, washed with methanol and dried, which was directly used for the next step without further purification.

5.1.2 General procedure for methyl 1,5-disubstituted-3-trifluoromethyl-1H-pyrazole (1-19)

A mixture of 1,3-dione adducts (0.05 mol) with selected substituted phenylhydrazines (0.06 mol) in ethanol or N,N-Dimethylformamide (DMF) (200 ml) was refluxed for 8 h. Water was then added after the reaction mixture was cooled down to room temperature. The resulting precipitate was collected and recrystallized from methanol to give target compounds.

5.2 Antifungal susceptibility assays

The antifungal activity of newly synthesized compounds was tested following a modification of previously described protocol [26]. Briefly, to 900 ml of double-distilled water was added 26 g of potato dextrose agar (PDA) to give PDA medium. The medium prepared was autoclaved at 120 °C for 20 min before cooled down to 55 °C. The compounds stock solutions in DMSO diluted by mixing with the medium to give final indicated concentrations were poured into petri dishes (9 cm diameter). A treatment with vehicle (DMSO) was included as reference, and three replicates were performed for each treatment. Each petri dish was inoculated with a mycelia disc (1 mm diameter) pin-picked from the margin of freshly prepared source colonies of the respective fungus growing on PDA medium. After incubation in the dark, all three diameters of the mycelium for each treatment were measured, averaged and converted to percentage activity relative to vehicle treatment.

5.3 Transcriptome profiling assay

The transcriptome profiling assay and data process was performed according to the discribed protocal of Yang [27] with minor modifications. Briefly, liquid cultures of *Fusarium graminearum* (PH-1) were grown in YEPD (yeast extract peptone dextrose medium) on a rotary shaker (175 rpm at 25 °C) for three days, The cultures was then added compound **12** with a final concentration of 30 µmol/L and incubated for 3 hours. Fresh mycelia were collected and washed three times with sterile deionized water. The

smaple were then immediately frozen and stored in liquid nitrogen until analysis. Total RNA was extracted from these materials using RNAiso Plus (Total RNA extraction reagent) (TaKaRa, Otsu, Japan). RNA purity was verified using a NanoPhotometer spectrophotometer (Implen, Westlake Village, CA, USA). RNA concentration was measured using a Qubit RNA Assay Kit in a Qubit 2.0 Fluorometer (Life Technologies, Grand Island, NY, USA). RNA integrity was assessed using the RNA Nano 6000 Assay Kit of the Bioanalyzer 2100 system (Agilent Technologies, Wilmington, DE, USA). Library construction, RNA-seq sequencing, Read mapping to the reference genome, Differential expression analysis and Gene Ontology (GO) enrichment analysis all followed the protocol of Yang[27].

Acknowledgments

This work was supported by special fund from Henan Academy of Agricultural Sciences (Grant No. 20188109).

Reference

[1] R.A. Dean, N.J. Talbot, D.J. Ebbole, M.L. Farman, T.K. Mitchell, M.J. Orbach, M. Thon, R. Kulkarni, J.R. Xu, H. Pan, N.D. Read, Y.H. Lee, I. Carbone, D. Brown, Y.Y. Oh, N. Donofrio, J.S. Jeong, D.M. Soanes, S. Djonovic, E. Kolomiets, C. Rehmeier, W. Li, M. Harding, S. Kim, M.H. Lebrun, H. Bohnert, S. Coughlan, J. Butler, S. Calvo, L.J. Ma, R. Nicol, S. Purcell, C. Nusbaum, J.E. Galagan, B.W. Birren, The genome sequence of the rice blast fungus *Magnaporthe grisea*, *Nature*, 434 (2005) 980-986.

- [2] T.E. Motaung, H. Saitoh, T.J. Tsilo, Large-scale molecular genetic analysis in plant-pathogenic fungi: a decade of genome-wide functional analysis, *Mol Plant Pathol*, 18 (2017) 754-764.
- [3] <http://www.fao.org/faostat/en/#data/RP>, in, 2016.
- [4] C. Albertini, M. Gredt, P. Leroux, Mutations of the β -Tubulin Gene Associated with Different Phenotypes of Benzimidazole Resistance in the Cereal Eyespot Fungi *Tapesia yallundae* and *Tapesia acuformis*, *Pesticide Biochemistry and Physiology*, 64 (1999) 17-31.
- [5] G.A. Bardas, T. Veloukas, O. Koutita, G.S. Karaoglanidis, Multiple resistance of *Botrytis cinerea* from kiwifruit to SDHIs, QoIs and fungicides of other chemical groups, *Pest Manag Sci*, 66 (2010) 967-973.
- [6] R. Childers, G. Danies, K. Myers, Z. Fei, I.M. Small, W.E. Fry, Acquired Resistance to Mefenoxam in Sensitive Isolates of *Phytophthora infestans*, *Phytopathology*, 105 (2015) 342-349.
- [7] A.C. Klosowski, L.L. May De Mio, S. Miessner, R. Rodrigues, G. Stammler, Detection of the F129L mutation in the cytochrome b gene in *Phakopsora pachyrhizi*, *Pest Manag Sci*, 72 (2016) 1211-1215.
- [8] D.A. Pereira, B.A. McDonald, P.C. Brunner, Mutations in the CYP51 gene reduce DMI sensitivity in *Parastagonospora nodorum* populations in Europe and China, *Pest Manag Sci*, 73 (2017) 1503-1510.
- [9] M.F. Khan, M.M. Alam, G. Verma, W. Akhtar, M. Akhter, M. Shaquiquzaman, The therapeutic voyage of pyrazole and its analogs: A review, *European Journal of Medicinal Chemistry*, 120 (2016) 170-201.
- [10] S.G. Küçükgülzel, S. Şenkardes, Recent advances in bioactive pyrazoles, *European Journal of Medicinal Chemistry*, 97 (2015) 786-815.
- [11] A.A. Bekhit, T. Abdel-Aziem, Design, synthesis and biological evaluation of some pyrazole derivatives as anti-inflammatory-antimicrobial agents, *Bioorganic & Medicinal Chemistry*, 12 (2004) 1935-1945.
- [12] T.D. Penning, J.J. Talley, S.R. Bertenshaw, J.S. Carter, P.W. Collins, S. Docter, M.J. Graneto, L.F. Lee, J.W. Malecha, J.M. Miyashiro, R.S. Rogers, D.J. Rogier, S.S. Yu, AndersonGd, E.G. Burton, J.N. Cogburn, S.A. Gregory, C.M. Koboldt, W.E. Perkins, K. Seibert, A.W. Veenhuizen, Y.Y. Zhang, P.C. Isakson, Synthesis and biological evaluation of the 1,5-diarylpyrazole class of cyclooxygenase-2 inhibitors: identification of 4-[5-(4-methylphenyl)-3-(trifluoromethyl)-1H-pyrazol-1-yl]benzenesulfonamide (SC-58635, celecoxib), *J Med Chem*, 40 (1997) 1347-1365.
- [13] Y. Ma, S. Liang, Y. Zhang, D. Yang, R. Wang, Development of anti-fungal pesticides from protein kinase inhibitor-based anticancer agents, *Eur J Med Chem*, 148 (2018) 349-358.
- [14] Y. Ma, S.K. McCarty, N.P. Kapuriya, V.J. Brendel, C. Wang, X. Zhang, D. Jarjoura, M. Saji, C.S. Chen, M.D. Ringel, Development of p21 activated kinase-targeted multikinase inhibitors that inhibit thyroid cancer cell migration, *J Clin Endocrinol Metab*, 98 (2013) E1314-1322.

- [15] H.C. Chiu, J. Yang, S. Soni, S.K. Kulp, J.S. Gunn, L.S. Schlesinger, C.S. Chen, Pharmacological exploitation of an off-target antibacterial effect of the cyclooxygenase-2 inhibitor celecoxib against *Francisella tularensis*, *Antimicrob Agents Chemother*, 53 (2009) 2998-3002.
- [16] H.C. Chiu, S.L. Lee, N. Kapuriya, D. Wang, Y.R. Chen, S.L. Yu, S.K. Kulp, L.J. Teng, C.S. Chen, Development of novel antibacterial agents against methicillin-resistant *Staphylococcus aureus*, *Bioorg Med Chem*, 20 (2012) 4653-4660.
- [17] H.C. Chiu, S.K. Kulp, S. Soni, D. Wang, J.S. Gunn, L.S. Schlesinger, C.S. Chen, Eradication of intracellular *Salmonella enterica* serovar Typhimurium with a small-molecule, host cell-directed agent, *Antimicrob Agents Chemother*, 53 (2009) 5236-5244.
- [18] S. Thangamani, W. Younis, M.N. Seleem, Repurposing celecoxib as a topical antimicrobial agent, *Front Microbiol*, 6 (2015) 750.
- [19] J. Zhu, X. Song, H.P. Lin, D.C. Young, S. Yan, V.E. Marquez, C.S. Chen, Using cyclooxygenase-2 inhibitors as molecular platforms to develop a new class of apoptosis-inducing agents, *J Natl Cancer Inst*, 94 (2002) 1745-1757.
- [20] P.A.T. Pereira, B.C. Trindade, A. Secatto, R. Nicolete, C. Peres-Buzalaf, S.G.o. Ramos, R. Sadikot, C.d.S. Bitencourt, L.c.H. Faccioli, Celecoxib improves host defense through prostaglandin inhibition during *Histoplasma capsulatum* infection, *Mediators Inflamm*, 2013 (2013) 950981-950981.
- [21] T.T. Ashburn, K.B. Thor, Drug repositioning: identifying and developing new uses for existing drugs, *Nature Reviews Drug Discovery*, 3 (2004) 673-683.
- [22] C.R. Chong, D.J. Sullivan Jr, New uses for old drugs, *Nature*, 448 (2007) 645.
- [23] T. Shankar, M. Haroon, Y. Waleed, N.S. Mohamed, Drug Repurposing for the Treatment of Staphylococcal Infections, *Current Pharmaceutical Design*, 21 (2015) 2089-2100.
- [24] S. Thangamani, H. Mohammad, W. Younis, M.N. Seleem, Drug repurposing for the treatment of staphylococcal infections, *Curr Pharm Des*, 21 (2015) 2089-2100.
- [25] M.M. Ahlstrom, M. Ridderstrom, I. Zamora, K. Luthman, CYP2C9 structure-metabolism relationships: optimizing the metabolic stability of COX-2 inhibitors, *J Med Chem*, 50 (2007) 4444-4452.
- [26] R. Zeun, G. Scalliet, M. Oostendorp, Biological activity of sedaxane---a novel broad-spectrum fungicide for seed treatment, *Pest Manag Sci*, 69 (2013) 527-534.
- [27] L. Yang, L. Xie, B. Xue, P.H. Goodwin, X. Quan, C. Zheng, T. Liu, Z. Lei, X. Yang, Y. Chao, C. Wu, Comparative transcriptome profiling of the early infection of wheat roots by *Gaeumannomyces graminis* var. *tritici*, *PLoS One*, 10 (2015) e0120691.

Highlight

- Cyclooxygenase-2 (COX-2) selective inhibitor, celecoxib, was found directly inhibiting the growth of phytopathogenic fungi at concentrations over 100 µg/ml.
- Derivation of celecoxib leads to the identification of compound 12, a non-COX-2 inhibitor with increased antifungal activity.
- Transcriptome profiling analysis of compound 12 treated *Fusarium graminearum* (PH-1) revealed 406 up-regulated and 572 down-regulated differentially expressed genes (DEGs) respectively.
- These DEGS were enriched and cofactor binding was the most enriched gene ontology (GO) category.